PCCP

Accepted Manuscript

ROYAL SOCIETY OF CHEMISTRY

www.rsc.org/pccp

Energy & Environmental Science RSCPublishing

ARTICLE

Organic hydrophilic dye for water-based dye-sensitized solar cells

Cite this: DOI: 10.1039/x0xx00000x

V. Leandri,[a,b] H. Ellis,[b] E. Gabrielsson,[c] L. Sun,[c,d] G. Boschloo,[*b] A. Hagfeldt[b]

Received 00th January 2012,
Accepted 00th January 2012

DOI: 10.1039/x0xx00000x

www.rsc.org/

In this study we report the first organic hydrophilic dye employed for 100% water-based electrolyte DSSC. We show that the replacement of alkyl by glycolic chains on the dye structure is able to provide excellent wettability, resulting in an efficient system with remarkably reduced desorption problems that allowed us to perform tests on a wide pH range. By changing the electrolyte composition, employing chenodeoxycholic acid as co-adsorbent and using PEDOT counter-electrodes, 3% power conversion efficiency under 1-sun illumination, was reached. We show that chenodeoxycholic acid does not significantly increase the wettability, and we provide new insights on the higher performance resulting from its co-adsorption.

Broader Context

Dye-Sensitized Solar Cells (DSSCs) are part of the last generation solar cells consisting of organic and inorganic materials. Inspired by the natural process of the photosynthesis performed with organic pigments in plant organisms, DSSC have always been considered an environmentally friendly technology. However, in order to reach higher performances, liquid electrolytes based on toxic and flammable organic solvents and additives have been employed. Recently, several efforts to fabricate devices based on water-electrolytes have been made. In this work, we report a very simple and environmentally friendly system, able to yield good performances. We propose a new approach consisting in a modification of the dye properties that allow us to avoid any additive in the electrolyte. Currently, this is the first device employing counter electrodes electropolymerized in water and a 100% water electrolyte containing no additives, to yield good performances. Therefore, this work can be considered as a concrete leap forward in the direction of simple and environmentally friendly generation of devices.

Introduction

Dye-Sensitized Solar Cells (DSSCs) are considered one of the most promising photovoltaic devices due to their low fabrication cost and high versatility.[1,2,3,4] The most common DSSCs architecture consists of a dye-stained TiO_2 film and a Pt counter electrode, assembled into sealed sandwich-type cells. The electrodes are bridged through a liquid electrolyte, whose composition play a fundamental role in the device performances. The idea of photovoltaic devices based on chromophores adsorbed on TiO_2 was born in the 1980s, from studies on the same electrode as photocatalyst for methane production and photodecomposition of aqueous liquids, in visible light.[5,6,7] Therefore, the photovoltaic pioneering studies were naturally oriented in the direction of aqueous media.[8,9,10] However, the inclusion of water in DSSCs have been later ascribed to significantly lower the efficiency, and water-soluble dyes, such as the ruthenium complexes initially developed, required pH 3 buffer solutions in order to be firmly anchored on the TiO_2 surface without desorbing. Therefore, water was quickly replaced by organic solvents, able to provide much higher performances that made DSSCs a promising candidate for future commercialization.[1,11,12,13] Furthermore, many efforts have been made to produce sealing agents for complete isolation against moisture.[14,15] However, highly performing DSCs employ liquid electrolytes based on organic solvents and additives usually inflammable and hazardous both for human health and the environment. Therefore, the idea of an efficient,

a Department of Materials Science, University of Milano-Bicocca, Via Cozzi 53, 20125 Milano, Italy
b Physical Chemistry, Centre of Molecular Devices, Department of Chemistry-Angstrom, Uppsala University (UU), SE-751 20 Uppsala, Sweden, E-mail: gerrit.boschloo@fki.uu.se
c Organic Chemistry, Centre of Molecular Devices, Department of Chemistry, School of Chemical Science and Engineering, KTH Royal Institute of Technology, SE-100 44, Stockholm, Sweden
d State Key Laboratory of Fine Chemicals, DUT-KTH Joint Research Center on Molecular Devices, Dalian University of Technology (DUT), 116024 Dalian, China.

inexpensive, simple, and environmentally friendly system based on water, results still attractive and is pushing the research back in this direction.[16,17,18] DSSCs with remarkable results, based on 100% water electrolytes, have been recently reported by O'Regan *et al.* and Spiccia *et al.*[19,20,21] Up to-date, the common approach to water-electrolytes DSCs, is based on the use of hydrophobic dyes, to prevent desorption problems.[16,18,19,20] This strategy implies the employment of surfactants in the electrolyte solution to provide sufficient pore wettability, for a good interaction with the dye. However, such additives must be introduced in considerable amount, complicating the system and possibly resulting in mass transport problems. Currently, the reported $[Co(bpy)_3](NO_3)_2$ complex is scarcely soluble in water and the ferricyanide-based cells need a blocking layer in order to yield good efficiency. Therefore, we decided to develop a very simple system based on a new approach, using the classical iodide/triiodide as redox couple. D35 is a well-known dye, developed by Sun *et al.*[22] Our new approach consisted in the synthesis of its hydrophilic analogous, by substituting the hydrophobic alkyl chains with glycolic ones. The resulting hydrophilic dye, V35, shows an extraordinary interaction with water that allowed us to avoid the use of surfactants, without being affected by the same critical desorption issue of water-soluble ruthenium complexes.

Results and discussion

Optical and Electrochemical Characterization

Fig. 1 shows the molecular structures of the dyes involved in this study, D35 and V35. The synthetic route for V35 is reported in detail in the ESI (Scheme S1).

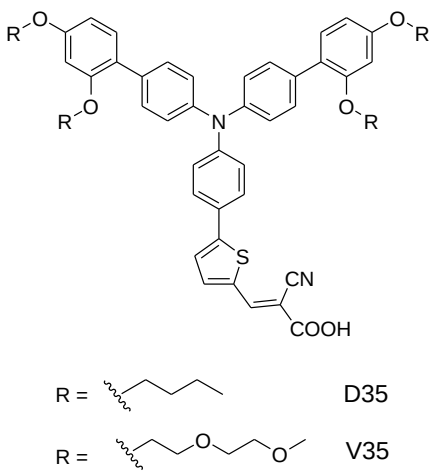

Fig. 1 Molecular structures of hydrophobic dye (D35) and hydrophilic dye (V35).

V35 has been optically and electrochemically characterized to study any possible alteration of such properties with respect to D35, deriving from the use of different chains. Uv-Vis absorption and emission spectra in CH_2Cl_2 of the dyes are reported in Fig. 2. Both dyes exhibit one absorption band in the visible region at 495 and 503 nm for V35 and D35, respectively, related to the intramolecular charge transfer (ICT). Therefore, the dyes slightly differ in terms of maximum absorption and emission wavelengths. In particular, dye V35 exhibits a slightly hypsochromically shifted absorption spectrum and bathochromically shifted emission spectrum, with respect to D35.

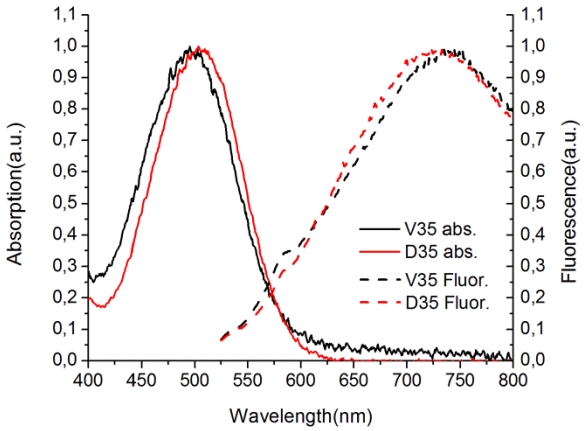

Fig. 2 Normalized absorption (left) and emission (right) spectra of V35 (black lines) and D35 (red lines), recorded in CH_2Cl_2.

The main optical parameters of V35 and D35, together with HOMO and LUMO levels derived from cyclic voltammetry in CH_3CN (ESI, Fig. S2) and the energy bandgap, estimated from interception of absorption and emission spectra, are collected in Table 1.

Table 1 Main optical and electrochemical parameters of dyes V35 and D35.

Dye	λ_{abs} (nm)[a]	λ_{emiss} (nm)[a]	ε ($M^{-1}cm^{-1}$)[a]	E_{HOMO} (NHE)[b]	E_{LUMO} (NHE)[d]	$E_{0\text{-}0}$ (eV)[c]
V35	495	722	27500	1.07	-1.11	2.18
D35	503	740	31000[e]	1.04	-1.12	2.16

[a]Recorded in CH_2Cl_2, [b]Measured by CV (V35 0.2 mM, $LiClO_4$ 0.1 M in CH_3CN) vs Ag/Ag+. Reference electrode calibrated against an internal Fc/Fc+ reference (using E°(Fc/Fc+) = 0.63 V vs NHE), [c]Estimated from the interception of the normalized absorption and emission spectra, [d]Estimated by subtracting $E_{0\text{-}0}$ from the oxidation potential, [e]Value reported in literature.[23]

In addition to the slightly shifted spectra, V35 exhibits a relatively lower molar extinction coefficient, indicating a reduced ability to harvest light deriving from the glycolic chains. Electrochemical measurements reflect the optical observations, showing that the HOMO level of both dyes are located at slightly different energies. A very small difference is also observed in the values of the optical bandgap and, consequently, of the LUMO level.

Photovoltaic investigation in DSSCs

The new dye V35 has been tested in DSSCs to explore its characteristics with respect to D35. Initial tests were operated

employing an electrolyte composed by NaI and I_2 in 100% deionized water and, gradually, modifications were introduced. The experiments initially performed and the detailed photovoltaic parameters are reported in Table 2.

Table 2 Detailed photovoltaic parameters of initial tests.

Dye	Electrolyte	J_{sc}(mAcm^{-2})	V_{oc}(mV)	FF(%)	η(%)
V35	2 M NaI, 20 mM I_2[a]	2.30	500	67	0.80
	2 M KI, 20 mM I_2 [a]	4.07	550	70	1.55
	2 M KI, 20 mM I_2, pH 4.0[b]	3.72	515	73	1.40
	4 M KI, 20 mM I_2 [a]	4.78	570	65	1.76
D35	2 M NaI, 20 mM I_2 [a]	0.11	350	55	0.02
	2 M KI, 20 mM I_2 [a]	0.11	375	54	0.05
	4 M KI, 20 mM I_2 [a]	0.34	440	46	0.07

[a] Deionized water; [b]buffer solution.

Significant enhancement of the power conversion efficiency is recorded for V35, when KI replaces NaI in the electrolyte composition. Although this aspect has not been further investigated, it is possible to speculate that is probably related to the ability of glycolic chains, like crown ethers, to coordinate small cations, such as Na^+.[24,25] The decrease in open-circuit voltage collected in pH 4.0 buffer solution, is due to the polarization induced on the surface by H^+ ions, that shifts positively the potential of the CB of TiO_2.[26] Additionally, this lower efficiency shows that the acidic conditions, necessary to test ruthenium complexes in aqueous solutions, are not suitable for V35, confirming its stability on the surface. The further improvement, observed by doubling the concentration of KI, is probably due to the further shift in the equilibrium that suppresses free iodine concentration.[19] Finally, it should be noticed that, under these conditions, no photocurrent was recorded in the devices fabricated employing D35.

Since it has been reported that guanidinium salts and chenodeoxycholic acid (CDCA) act as surfactants,[19] their effects on this system were investigated. Table 3 collects the performed experiments.

Table 3 DSSCs parameters investigating GuSCN and CDCA effects.

Dye	Electrolyte	J_{sc}(mAcm^{-2})	V_{oc}(mV)	FF(%)	η(%)
V35	4 M KI, 20 mM I_2, 0.2 GuSCN	3.83	550	68	1.42
	4 M KI, 20 mM I_2, 0.5 GuSCN	3.33	555	67	1.25
D35	4 M KI, 20 mM I_2, 0.5 GuSCN	1.43	532	61	0.46
V35	2 M KI, 20 mM I_2, 0.2 GuSCN	3.22	545	68	1.20
	2 M KI, 20 mM I_2, 0.5 GuSCN	2.32	550	69	0.89
D35	2 M KI, 20 mM I_2, 0.5 GuSCN	0.10	488	46	0.23
V35	4 M KI, 20 mM I_2, cdca[a]	4.86	600	76	2.20
D35	4 M KI, 20 mM I_2, cdca[a]	0.63	580	77	0.28
V35	4 M KI, 20 mM I_2, 0.5 GuSCN, cdca[a]	4.71	582	66	1.81
D35	4 M KI, 20 mM I_2, 0.5 GuSCN, cdca[a]	2.15	581	65	0.81

Photovoltaic parameters of DSSCs employing Pt counter electrodes. [a]Working electrode sensitized 1:50=dye:CDCA, electrolyte solution in deionized water saturated with CDCA.

The reported data show a different response of the dyes to GuSCN. The addition of GuSCN in the electrolyte composition has a negative effect in combination with V35, but a positive impact on the hydrophobic D35. Indeed, by making a comparison between these results and the one recorded without GuSCN, is evident that this component mainly affects the J_{sc} values, causing lower efficiency for V35, and higher for D35. On the other hand, the co-sensitization with CDCA results in a positive effect for both dyes. The combination of the two components does not result in a synergistic effect on V35, reflecting the negative influence of GuSCN. Different results are collected for hydrophobic D35, which exhibits a synergistic effect deriving from both GuSCN and CDCA. However, the data suggest that, employed singularly, the guanidinium salt (in this low concentration) and chenodeoxycholic acid are able to provide only slightly wetting, associated with the improved performances of D35. Furthermore, it should be pointed out that the synergistic effect on D35, is still not able to exceed the results obtained with V35.

Due to recent improvements reached with electro-polymerized PEDOT counter electrodes on FTO glass,[27] a comparison between platinum and PEDOT was made (Table 4). From Table 4 is evident that PEDOT counter electrodes, outperform the platinum ones due to the increased photocurrent and open circuit voltage. Both PEDOT and platinum counter electrodes exhibit total wetting upon deposition of water on the surface, therefore the increased photocurrent cannot be explained in terms of wettability. We attributed this result to the leaf-like PEDOT structure that confers high-surface area, leading to an increase in the catalytic activity. In addition, it is important to notice that we observed a reduced tendency of the dye to desorb, when PEDOT counter electrodes were used. We did not further investigate this phenomenon but we speculated it can be reasonably due to the ability of PEDOT to include ions in its matrix.[28,29] Indeed, we often noticed a slight desorption after a few days when platinum counter electrodes were used, however, we surprisingly did not observe the same phenomenon when PEDOT was employed. We believe that PEDOT partially trapped in its matrix the ions able to absorb on the surface of TiO_2, preventing in this way the desorption of the dye.

Table 4 Photovoltaic parameters of DSSCs with different counter electrodes.

Dye	Electrolyte	J_{sc}(mAcm^{-2})	V_{oc}(mV)	FF(%)	η(%)
V35	4 M KI, 20 mM I_2[b]	4.78	570	65	1.76
	4 M KI, 20 mM I_2, cdca[a, b]	4.86	600	76	2.20
	2 M KI, 20 mM I_2, 0.5 GuSCN[b]	2.32	550	69	0.89
	4 M KI, 20 mM I_2[c]	5.17	590	68	2.06
	4 M KI, 20 mM I_2, cdca[a, c]	5.26	625	74	2.45
	2 M KI, 20 mM I_2, 0.5 GuSCN[c]	3.35	540	71	1.29
D35	4 M KI, 20 mM I_2, cdca[a, b]	0.63	580	77	0.28
	4 M KI, 20 mM I_2, cdca[a, c]	1.18	605	61	0.44

[a]Working electrode sensitized 1:50= dye:CDCA, electrolyte solution: deionized water saturated with CDCA, [b]DSSCs with Pt counter electrodes; [c]DSSCs with PEDOT counter electrodes.

Finally, PEDOT counter electrodes represent a cheaper and environmental friendly alternative to platinum, as they are fabricated from cheap materials and the electropolymerization is carried out at room temperature, in deionized water.

In order to compare the achieved results with a performing electrolyte, dyes V35 and D35 were tested with the best electrolyte reported by O'Regan *et al*. (Table 5).[19]

Table 5 Photovoltaic parameters of DSSCs employing O'Regan's electrolyte and PEDOT counter electrodes.

Dye	Electrolyte	J_{sc}(mAcm^{-2})	V_{oc}(mV)	FF(%)	η(%)
V35	8 M GuI, 20 mM I_2	3.77	500	61	1.16
	8 M GuI, 20 mM I_2, cdca[a]	5.76	550	62	1.97
D35	8 M GuI, 20 mM I_2	3.13	500	63	1.00
	8 M GuI, 20 mM I_2, cdca[a]	5.89	520	64	1.95

[a]Working electrode sensitized 1:50=dye:CDCA, electrolyte solution: deionized water saturated with CDCA.

Data reported in Table 5 show that by using very high concentration of guanidinium salt, great wettability is achieved and both hydrophilic and hydrophobic dyes perform similarly. However, elevate concentration of guanidinium salts decreases significantly the V_{oc} due to the absorption of guanidinium cations on the surface of TiO_2.[30] Measurements performed with and without CDCA show, once again, its remarkable impact on the performances. However, a comparison between the efficiency reported in Tables 5 and 4, confirms that the approach based on a hydrophilic dye that does not need surfactants, yields better efficiency.

Further optimization of iodine and CDCA concentrations, yielded the highest efficiency recorded with V35 (Table 6). It should be stressed that the efficiency achieved, 3% under 1 sun (4% under 0.5 sun) illumination, is perfectly in line with the state-of-the-art for D35-modified dyes in water systems.[18] However, in the study presented here, no additives and no ionic liquids are employed, confirming the validity of this approach.

Table. 6 Photovoltaic parameters of best performing DSSCs employing V35 dye, with PEDOT counter electrodes.

Dye	Electrolyte	J_{sc}(mAcm^{-2})	V_{oc}(mV)	FF(%)	η(%)
V35	2 M KI, 10 mM I_2, cdca[a]	6.85	650	67	3.01[b]
	2 M KI, 10 mM I_2, cdca[a]	4.16	635	70	4.04[c]

[a]Working electrode sensitized 1:15=dye:CDCA, electrolyte solution: neutral water saturated with CDCA, [b]Measured under 1 sun illumination; [c]Measured under 0.5 sun illumination.

Lower iodine concentration significantly improved the V_{oc} value. However, concentrations lower than 10 mM resulted in very low current. The concentration of CDCA must be well balanced as well, as higher concentration led to higher open-circuit voltage, but lower photocurrent, due to the reduced amount of dye absorbed on the surface.

Interesting insights on the role of CDCA can be found in the IPCE and electron lifetime measurements of the most significant experiments (Figure 3).

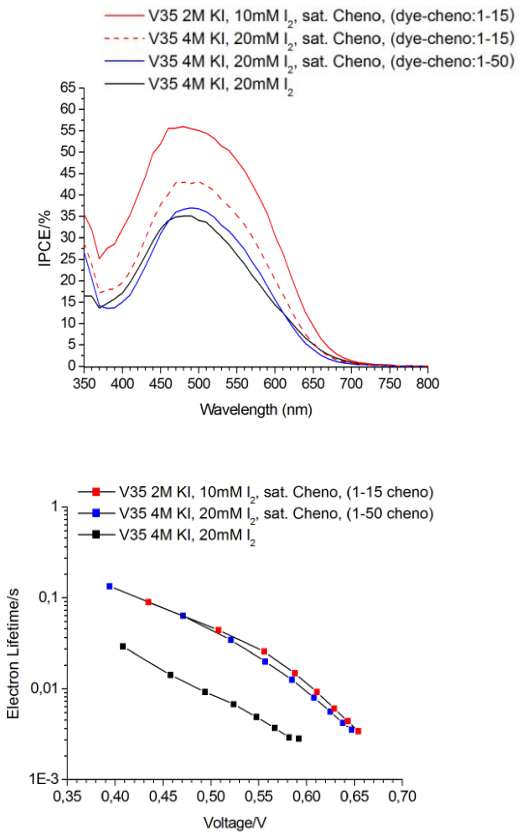

Fig. 3 IPCE spectrum (top) and Electron Lifetime (bottom) of main DSSC from this study, with PEDOT counter electrodes.

The comparison of data recorded with and without CDCA, show its remarkable impact on the electron lifetime. Parallel to this, we observed a significant enhancement of the V_{oc} when CDCA is co-adsorbed on the surface of TiO_2. Since CDCA does not shift significantly the conduction band of TiO_2,[31] we can state that the data indicate a reduction of the recombination processes.

As previously reported (Table 2), the experiment performed in acidic buffer solution resulted in lower efficiency. Therefore, we decided to explore the behaviour of the system in basic conditions employing an electrolyte composed by 4 M KI and 20 mM I_2 in pH 8.0 and pH 9.0 buffer solutions. Figure 4 shows the variation of the photovoltaic parameters recorded, over a period of 18 days. The cells were stored in the dark and measured in the reported days. Both V_{oc} and FF are higher in the case of buffer at pH 9.0, however, this is compensated by a lower photocurrent, that globally lowers the efficiency with respect to the pH 8.0 buffer. Interestingly, V_{oc} considerably increases over time in all the devices fabricated. It is very important to notice that this latter aspect was also exhibited by all the DSSCs of this study. Indeed, it should be specified that the photovoltaic parameters of all the cells in this study were subjected to fluctuations over time and the values reported in the tables were collected after several days after devices assembly.

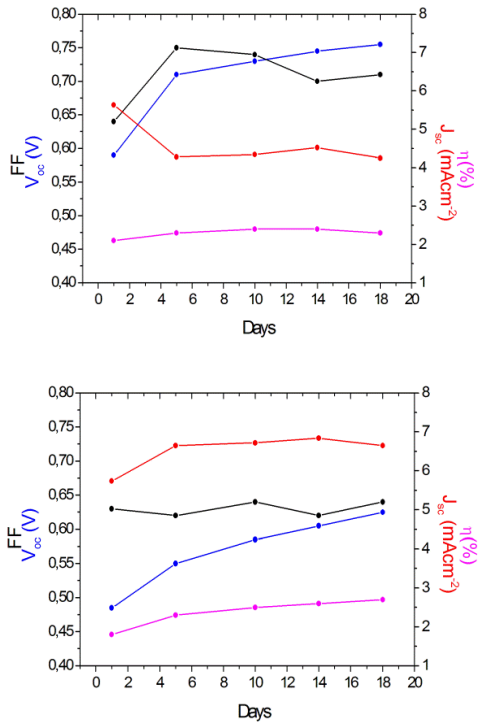

Fig. 4 Photovoltaic performance parameters of DSSCs with electrolyte: 4M KI, 20 mM I_2, pH 9.0 buffer solution (top); and electrolyte: 4M KI, 20 mM I_2, pH 8.0 buffer solution (bottom). PEDOT counter electrodes were used.

Table 7 reports the detailed photovoltaic parameters of the best performing cells from the pH study.

Table. 7 Photovoltaic parameters of the best DSSCs employing pH 9 and pH 8 electrolyte solutions.

Dye	Electrolyte	J_{sc}(mAcm^{-2})	V_{oc}(mV)	FF(%)	η(%)
V35	4 M KI, 20 mM I_2, pH 9.0[c]	4.52	745	70	2.4[a]
	4 M KI, 20 mM I_2, pH 8.0[c]	6.65	625	64	2.7[b]

[a]After 14 days; [b]After 18 days; [c]Buffer solution.

A comparison between the results reported in Table 7 and the efficiency collected in Table 4, clearly show that the employment of pH 8.0 buffer yields better performance. Since we previously showed a great enhancement of the performances arising from a co-sensitization with CDCA, we fabricated devices using the same technique and the pH 8.0 buffer electrolyte solution reported. However, in this case, we collected lower efficiency. We did not further investigate this result, but a possible explanation may reside in the fact that CDCA is more soluble in basic solutions rather than in neutral deionized water, and desorption may occur.

Contact Angle

A critical aspect in water-based electrolytes for DSSCs is the pore wettability.[19] High interfacial contact between the dye and the aqueous electrolyte is essential for efficient dye regeneration and, consequently, good performances. In order to test the properties of V35 and D35 in terms of hydrophilicity/hydrophobicity, measurements of the contact angles (Θ_c) were performed. The results show a remarkably different interaction of the dyes with water (Fig. 5).

D35 /H_2O, Θ_c = 124° V35/H_2O, Θ_c = 41°

Fig. 5 Crossed sections of working electrodes sensitized with D35 (left) and V35 (right) with a drop of deionized water positioned on the top. The pictures, used for the estimation of the contact angles (Θc), reflect the hydrophobicity of D35 and hydrophilicity of V35.

Contact angles > 90° indicate hydrophobic character, while values < 90° denote hydrophilic properties of the surface in exam. Therefore, the hypothesis that V35 can provide an excellent surface interaction with aqueous media, have been totally validated.

Further investigation on the influence of CDCA on the hydrophilicity/hydrophobicity was made by measuring the contact angle of working electrodes co-sensitized with different amount of CDCA (Table 8).

Table. 8 Contact angles measurements with different amount of co-adsorbed CDCA and electrolyte compositions.

Dye/ Dye:CDCA	Electrolyte	Contact Angle (Θ_c/°)
V35	water[a]	41
D35	water[a]	124
V35/ 1:5	water[a]	31
D35/ 1:5	water[a]	121
V35/ 1:15	water[a]	34
D35/ 1:15	water[a]	111
V35/ 1:50	water[a]	26
D35/ 1:50	water[a]	104
V35/ 1:5	2 M KI, 10 mM I_2, cdca[b]	16
D35/ 1:5	2 M KI, 10 mM I_2, cdca[b]	98
V35/ 1:15	2 M KI, 10 mM I_2, cdca[b]	22
D35/ 1:15	2 M KI, 10 mM I_2, cdca[b]	91
V35/ 1:50	2 M KI, 10 mM I_2, cdca[b]	15
D35/ 1:50	2 M KI, 10 mM I_2, cdca[b]	90
V35	2 M KI, 10 mM I_2[a]	41
D35	2 M KI, 10 mM I_2[a]	91
V35	4 M KI, 10 mM I_2[a]	43
D35	4 M KI, 10 mM I_2[a]	84
D35	8 M GuI, 20 mM I_2[a]	77[c]
V35	8 M GuI, 20 mM I_2[a]	0

[a]Deionized water, [b]Deionized water saturated with CDCA, [c]After short time total wetting was observed.

In particular, co-sensitizing TiO_2 with a ratio 1:50/dye:CDCA lowers the value of contact angle of only 15° in the case of V35, and 20° in the case of D35. These results are consistent with the data collected in Table 3, where the 1:50/D35:CDCA

ratio does not provide a sufficient wettability for efficient current flowing and good performance. On the other hand, the electrolyte employing 8 M of GuI is able to provide total wetting for both dyes.

Photo-induced Absorption Spectroscopy (PIA)

In order to complete the photovoltaic cycle by restoring the electroneutrality of the dye, the interaction between the sensitizer and the electrolyte solution is crucial. The remarkable wettability induced by the glycolic chains is reflected in the photo-induced absorption measurements (Figures 6-8).

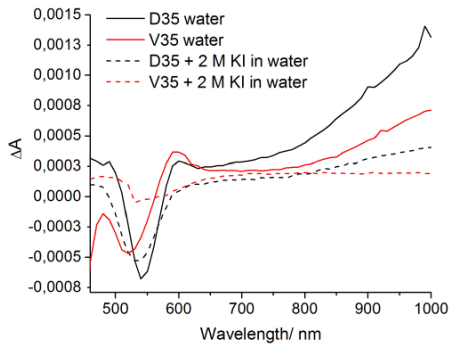

Figure 6 Photo-induced absorption spectra of V35 and D35 dyes in water, and in water/2 M KI in water electrolytes.

PIA measurements were not performed with full electrolyte composition as iodine seems to shift the spectra. Figure 6 shows that V35 is fully regenerated by the electrolyte. The V35/water signal exhibits an absorption peak at 600 nm and a rising signal after approximately 780 nm, related to the absorption of the oxidized dye. When 2 M KI solution is employed, the signal turns flat and the absorption peaks at 600 nm and after 780 nm disappears, indicating reduction of the oxidized dye. D35 exhibits the same profile, however, when 2 M KI is added, the signal after 780 nm does not turn completely flat, indicating that the dye is not fully regenerated.

The effect of the co-adsorption with CDCA was also investigated with this technique (Figure 7).

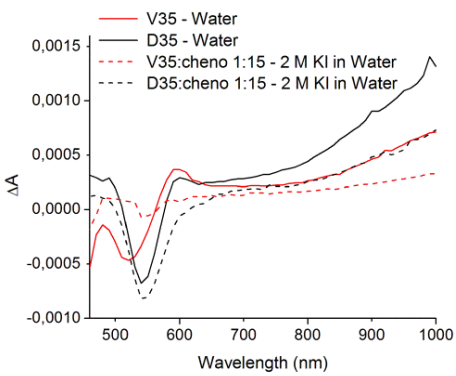

Figure 7 Photo-induced absorption spectra of V35 and D35 dyes in water, and co-sensitized with CDCA in water/2 M KI in water saturated with CDCA electrolytes.

V35, co-sensitized with CDCA reduces the absorption peak at 600 nm and the rise in absorption at above 780 nm. D35 shows still strong signals of its oxidized form.

Guanidinium salts have been recently employed with great success in 100% water-based DSSC.[19] We previously reported our investigation on the effect of the guanidinium salts on this water system (Tables 3 and 5). Figure 8 shows the PIA spectrum of V35 and D35 dyes employing a guanidinium iodide solution in water.

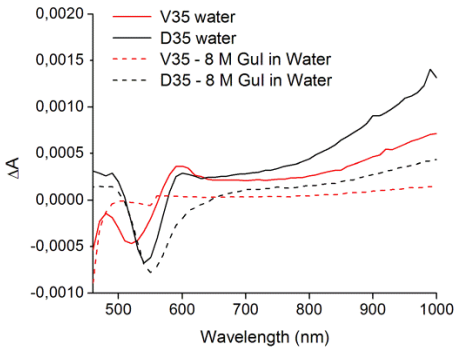

Figure 8 Photo-induced absorption spectra of V35 and D35 dyes with 8 M GuI in water solution.

Once again, the data show that V35 undergoes complete regeneration while D35, due to its hydrophobic alkoxyl chains, is still not fully regenerated.

A particularly interesting aspect arising from PIA measurements is that the dyes seem to give different Stark effects. In Figures 6-8 it is possible to see how the signal related to the Stark effect at around 550 nm is decreased, almost lost, when measuring V35 in combination with the iodide salts. On the other hands, the combination V35/Water and D35 do not show this behaviour. This difference may resides in the different mobilities of the ions in the different systems. However, this aspect was not further investigated.

Conclusions

In conclusion, a simple water-based system, based on the first organic dye bearing glycolic chains on the donor moiety, have been presented.

We have shown that the replacement of alkyl chains by glycolic ones does not result in a modification of the optical and electrochemical properties of the organic sensitizer V35, but it dramatically affect the hydrophilicity. By providing an excellent interaction at the dye/electrolyte solution interface with V35, we have been able to record good performances without the employment of additional surfactants. In contrast, hydrophobic dye D35 does not perform in absence of surfactant. A comparison with a highly performing electrolyte based on GuI, shows that in presence of a remarkable amount of surfactant, V35 and D35 perform very similarly. However, V35 is able to provide higher efficiency in combination with a simple electrolyte composition, without surfactants, confirming

the validity of the new approach. The results provided by photo-induced absorption measurements provide an additional confirmation to the fact that the glycolic chains provide good interaction with the water-based electrolyte, positively affecting the regeneration of the dye. On the other hand, the hydrophobic alkoxyl chains on D35 create problems for the redox couple to reach the hole, located on the triphenylamine unit, for regenerating the oxidized dye. The lower performances recorded by using acidic buffer solutions, and the good results obtained by employing basic pH buffer solutions, show a good stability of the dye on the surface of TiO_2 in contrast to the previously employed hydrophilic ruthenium complexes. In addition, we investigated the role of chenodeoxycholic acid, showing its negligible surfactant properties. From the data presented, we can firmly state that the remarkable improvements deriving from its co-adsorption are not due to the slightly increased wettability but are, more likely, connected to its ability to reduce recombination processes.

Experimental section

All chemicals were purchased from Sigma–Aldrich and used as received unless noted otherwise. FTO-coated glass substrates were purchased from Pilkington. TEC15 and TEC8 were used for working electrodes and counter electrodes, respectively.

Optical Characterization

Equipment used for the evaluation of the molar extinction coefficient: Jenway 6505 UV/Vis Spectrometer. Equipment used for other absorption measurements (desorption study in the ESI): UV-Vis NIR Light Source DH-2000-BAL from Mikropack used together with a spectrometer from Ocean Optics inc. (HR 2000 High Resolution spectrometer). The emission spectra were recorded using a Horiba Jobin Yvon Fluorolog with correction files for wavelength-dependent sensitivity of the instrument.

Fabrication of Dye-Sensitized Solar Cells

FTO glass substrates TEC15 were washed in ultrasonic bath for one hour in each of the following media: detergent, deionized water and ethanol. The glass substrates were pre-treated in a 40 mM aqueous $TiCl_4$ solution at 70°C for 90 min and then washed with water and ethanol. After drying in air the substrates were screen printed (active area 0.25 cm^2) one time with a Dyesol 18 NR-T paste, 20nm particle size (thickness around 3.0 μm after sintering). The substrates were dried at 125°C for 10 min before being screen-printed with a TiO_2-scattering paste (Solaronix Ti-Nanooxide R/SP). The samples (total thickness around 8 μm) were heated gradually at 180°C (10 min), 320°C (10 min), 390°C (10 min) and 500°C (60 min) in an oven (Nabertherm Controller P320) in air atmosphere. After sintering the samples were once again treated in 40 mM aqueous $TiCl_4$ at 70°C, for 30 min. A final heating step (500°C for 60 min) was performed. Before immersing the electrodes in the dye bath the electrodes were cooled to 90°C. The dye baths of V35 and D35 had a concentration of 0.2 mM in ethanol. The organic dye V35, (structure in Fig. 1) was developed in KTH-Stockholm (synthetic procedure in the ESI). The films were left in dye bath overnight (14 h) in the dark, rinsed with ethanol and assembled in a sandwich structure with the counter electrode. A 30 μm thick thermoplastic Surlyn frame was used (Meltonix 1170-25 from Solaronix). The electrolyte was introduced in the solar cells through one of the two predrilled holes, sealed with thermoplastic Surlyn cover and glass coverslip.

Preparation of Counter Electrodes

Predrilled two-holes TEC8 glass was washed in ultrasonic bath for one hour in each of the three following media; detergent (RBS25, 99%, Fluka), deionized water and ethanol (VWR DBH Prolabo, 99.9%). The solution for electropolymerization contained a micellar aqueous solution of 0.1 M SDS (>99% purity) and 0.01 M EDOT and was obtained by dissolving the SDS and EDOT in deionized water and ultrasonicating for one hour according to the method reported by Sakmeche et al.[32] Electropolymerization of EDOT was performed with an IviumStat.XR (Ivium Technologies) electrochemical instrument in the galvanostatic mode; a two-electrode cell with a 9 cm × 9 cm conducting glass as counter electrode and a predrilled washed 9 cm × 9 cm TEC8 glass as working electrode was used for this purpose, and a constant current of 13 mA was applied (the working electrode potential was about 1.22 V vs NHE). The PEDOT deposit was blue-colored (electropolymerization time: 320 sec).

Platinum counter electrodes (TEC8) were prepared by depositing 10 $\mu L cm^{-2}$ of a 4.8 mM H_2PtCl_6 solution in ethanol to the glass substrate followed by heating in air at 400°C for 30 min.

Characterization of Dye-Sensitized Solar Cells

Current–voltage (IV) measurements were carried out with a Keithley 2400 source/meter and a Newport solar simulator (model 91160); the light intensity was calibrated using a certified reference solar cell (Fraunhofer ISE), to an intensity of 1000 W m^{-2}. For the IV-measurements a black mask with an aperture of 0.5 cm × 0.5 cm was used in order to avoid significant additional contribution from light impinging on the device outside the active area (0.5 cm × 0.5 cm). The apparatus for incident photon to current conversion efficiency (IPCE) and electron lifetime measurements have been previously described.[33] The photo-induced absorption setup has been described in detail elsewhere.[34] The samples were excited by a blue LED (Luxeon Star 1 W, Blue, 470 nm), square-wave modulated (on/off) by using a HP 33120A waveform generator and a home-built LED driver system. The excitation light was superimposed on the white pump light provided by a 20 W tungsten-halogen lamp. The transmitted probe light was focused onto a monochromator (Acton Research Corporation SP-150) and detected using a UV-enhanced Si photodiode, connected to a lock-in amplifier via a current amplifier (Stanford Research Systems models 830 and 570, respectively). For time-resolved studies the output of the current amplifier

was connected to a data acquisition board (National Instruments PCI-6052E).

Contact angle

Images for contact angles measurements were collected employing a Dino-Lite Pro AM413T microscope. Elaboration of images was performed using Dinocapture 2.0 software. Working electrodes preparation followed the same general procedure previously reported. One active layer (total thickness around 3.0 μm after sintering) was screen-printed using Dyesol 18 NR-T paste, 20 nm particle size. The screen-printed electrodes were heated at 500°C, cooled down to 90°C and placed into the proper dye bath.

Acknowledgements

The authors would like to thank the Swedish Research Council, the Swedish Energy Agency, Knut and Alice Wallenberg Foundation and the STandUP energy program for financial support. We thank Dr. Bao-Lin Lee (Stockholm University) for the help with the HR-MS measurements.

Notes and references

† Electronic Supplementary Information (ESI) available: Synthesis and characterization of V35, CV measurement and V35 desorption spectra. See DOI: 10.1039/b000000x/

1. B. O'Regan and M. Grätzel, *Nature*, 1991, **353**, 737–739.
2. M. Wu, X. Lin, T. Wang, J. Qiu, and T. Ma, *Energy Environ. Sci.*, 2011, **4**, 2308.
3. Y. Li, D.-K. Lee, J. Y. Kim, B. Kim, N.-G. Park, K. Kim, J.-H. Shin, I.-S. Choi, and M. J. Ko, *Energy Environ. Sci.*, 2012, **5**, 8950.
4. S. Yoon, S. Tak, J. Kim, Y. Jun, K. Kang, and J. Park, *Build. Environ.*, 2011, **46**, 1899–1904.
5. E. Borgarello, J. Kiwi, E. Pelizzetti, M. Visca, and M. Grätzel, *Nature*, 1981, **289**, 158–160.
6. E. Borgarello, J. Kiwi, and E. Pelizzetti, *J. Am. Chem. Soc.*, 1981, **103**, 6324–6329.
7. K. Thampi, J. Kiwi, and M. Graetzel, *Nature*, 1987, **327**, 506–508.
8. M. Matsumura, S. Matsudaira, H. Tsubomura, M. Takata, and H. Yanagida, *Ind. Eng. Chem. Prod. Res. Dev.*, 1980, **19**, 415–421.
9. J. Desilvestro, M. Gratzel, L. Kavan, J. Moser, and J. Augustynski, *J. Am. Chem. Soc.*, 1985, **432**, 2988–2990.
10. N. Vlachopoulos, P. Liska, J. Augustynski, and M. Grätzel, *J. Am. Chem. Soc.*, 1988, **110**, 1216–1220.
11. M. Grätzel and K. Kalyanasundaram, *Curr. Sci.*, 1994, **66**, 706.
12. M. K. Nazeeruddin, P. Péchy, T. Renouard, S. M. Zakeeruddin, R. Humphry-Baker, P. Comte, P. Liska, L. Cevey, E. Costa, V. Shklover, L. Spiccia, G. B. Deacon, C. a Bignozzi, and M. Grätzel, *J. Am. Chem. Soc.*, 2001, **123**, 1613–24.
13. A. Yella, H.-W. Lee, H. N. Tsao, C. Yi, A. K. Chandiran, M. K. Nazeeruddin, E. W.-G. Diau, C.-Y. Yeh, S. M. Zakeeruddin, and M. Grätzel, *Science*, 2011, **334**, 629–34.
14. H. Arakawa, T. Yamaguchi, K. Okada, H. Matsui, T. Kitamura, and N. Tanabe, *Fujikura Tech. Rev.*, 2009, **38**, 55–60.
15. Y. Tropsha and N. Harvey, *J. Phys. Chem. B*, 1997, **5647**, 2259–2266.
16. W. H. Lai, Y. H. Su, L. G. Teoh, and M. H. Hon, *J. Photochem. Photobiol. A Chem.*, 2008, **195**, 307–313.
17. C. Law, S. C. Pathirana, X. Li, A. Y. Anderson, P. R. F. Barnes, A. Listorti, T. H. Ghaddar, and B. C. O'Regan, *Adv. Mater.*, 2010, **22**, 4505–9.
18. H. Tian, E. Gabrielsson, P. W. Lohse, N. Vlachopoulos, L. Kloo, A. Hagfeldt, and L. Sun, *Energy Environ. Sci.*, 2012, **5**, 9752.
19. C. Law, O. Moudam, S. Villarroya-Lidon, and B. O'Regan, *J. Mater. Chem.*, 2012, **22**, 23387.
20. T. Daeneke, Y. Uemura, N. W. Duffy, A. J. Mozer, N. Koumura, U. Bach, and L. Spiccia, *Adv. Mater.*, 2012, **24**, 1222–5.
21. W. Xiang, F. Huang, Y.-B. Cheng, U. Bach, and L. Spiccia, *Energy Environ. Sci.*, 2013, **6**, 121.
22. D. P. Hagberg, X. Jiang, E. Gabrielsson, M. Linder, T. Marinado, T. Brinck, A. Hagfeldt, and L. Sun, *J. Mater. Chem.*, 2009, **19**, 7232.
23. E. Gabrielsson, H. Ellis, S. Feldt, H. Tian, G. Boschloo, A. Hagfeldt, and L. Sun, *Adv. Energy Mater.*, 2013, **3**, 1647–1656.
24. R. C. White, J. E. Benedetti, A. D. Gonçalves, W. Romão, B. G. Vaz, M. N. Eberlin, C. R. D. Correia, M. a. De Paoli, and A. F. Nogueira, *J. Photochem. Photobiol. A Chem.*, 2011, **222**, 185–191.
25. C. Shi, S. Dai, K. Wang, X. Pan, L. Zeng, L. Hu, F. Kong, and L. Guo, *Electrochim. Acta*, 2005, **50**, 2597–2602.
26. Y. Liu, A. Hagfeldt, X. Xiao, and S. Lindquist, *Sol. Energy Mater. Sol. Cells*, 1998, **55**, 267–281.

27. H. Ellis, N. Vlachopoulos, L. Häggman, C. Perruchot, M. Jouini, G. Boschloo, and A. Hagfeldt, *Electrochim. Acta*, 2013, **107**, 45–51.

28. H.-S. Park, S.-J. Ko, J.-S. Park, J. Y. Kim, and H.-K. Song, *Sci. Rep.*, 2013, **3**, 2454.

29. V. Armel, J. Rivnay, G. Malliaras, and B. Winther-Jensen, *J. Am. Chem. Soc.*, 2013, **135**, 11309–13.

30. N. Kopidakis, N. R. Neale, and A. J. Frank, *J. Phys. Chem. B*, 2006, **110**, 12485–12489.

31. T. Marinado, M. Hahlin, X. Jiang, M. Quintana, E. M. J. Johansson, E. Gabrielsson, S. Plogmaker, D. P. Hagberg, G. Boschloo, S. M. Zakeeruddin, M. Grätzel, H. Siegbahn, L. Sun, A. Hagfeldt, and H. Rensmo, *J. Phys. Chem. C*, 2010, **114**, 11903–11910.

32. N. Sakmeche, J. J. Aaron, M. Fall, S. Aeiyach, M. Jouini, J. C. Lacroix, and P. C. Lacaze, *Chem. Commun.*, 1996, **24**, 2723–2724.

33. S. M. Feldt, E. a Gibson, E. Gabrielsson, L. Sun, G. Boschloo, and A. Hagfeldt, *J. Am. Chem. Soc.*, 2010, **132**, 16714–24.

34. G. Boschloo and A. Hagfeldt, *Inorganica Chim. Acta*, 2008, **361**, 729–734.